

# Journal of Materials Chemistry C

Accepted Manuscript



This is an *Accepted Manuscript*, which has been through the Royal Society of Chemistry peer review process and has been accepted for publication.

*Accepted Manuscripts* are published online shortly after acceptance, before technical editing, formatting and proof reading. Using this free service, authors can make their results available to the community, in citable form, before we publish the edited article. We will replace this *Accepted Manuscript* with the edited and formatted *Advance Article* as soon as it is available.

You can find more information about *Accepted Manuscripts* in the [Information for Authors](#).

Please note that technical editing may introduce minor changes to the text and/or graphics, which may alter content. The journal's standard [Terms & Conditions](#) and the [Ethical guidelines](#) still apply. In no event shall the Royal Society of Chemistry be held responsible for any errors or omissions in this *Accepted Manuscript* or any consequences arising from the use of any information it contains.

## Bio-inspired Sensors Based on Photonic Structures of *Morpho* Butterfly Wings: A Review

Qingsong Li,<sup>a</sup> Qi Zeng,<sup>a</sup> Lei Shi,<sup>b</sup> Xiaohua Zhang<sup>c</sup> and Ke-Qin Zhang\*<sup>a</sup>

Received 00th January 20xx,  
Accepted 00th January 20xx

DOI: 10.1039/x0xx00000x

www.rsc.org/

The *Morpho* butterfly's wings display beautiful, naturally-occurring iridescent colors that are produced by incident light interacting with periodic nanostructures on wing scales. This type of photonic structure has attracted a great amount of attention from international researchers; studies devoted to this structure have especially increased in recent years. Due to the development of research on nature-inspired bionic structures, as well as demand for high-efficient low-cost microfabrication techniques, understanding and replicating the mechanism of *Morpho* butterfly structural coloration have become increasingly significant. These sophisticated structures have many unique functions and can be used for many applications. This review summarizes recent progress in bio-inspired sensors based on the photonic structures of *Morpho* butterfly wings. Bio-inspired sensors for infrared radiation/thermal, pH, vapor etc. are discussed in detail, with particular focus on fabrication methods and operation mechanisms. Finally, the disadvantages and limitations that may limit the practical applications of bio-inspired sensors are presented and discussed.

### 1. Introduction

The *Morpho* butterfly is a special geotropical species found mostly in South America, Mexico, and Central America. Because of its unique bright structural color, it has been the subject of scientific curiosity for decades.<sup>1-4</sup> The research of this structural color is an important branch of physical optics, and plays an important role in technological advancements for both industry and commercial sectors.<sup>1, 5</sup> In recent years, advancements in microscopy technology such as Scanning Electron Microscope (SEM) and Transmission Electron Microscopy (TEM), have made it possible to observe and analyze the nanostructures of the *Morpho* butterfly wings at the nanoscale, or even smaller. It was discovered that the unique appearance of the butterflies' wings are a result of interference and diffraction of incident light, which interact with the nanoscale structures on the *Morpho* butterfly wings to produce bright and iridescent colors.<sup>6-8</sup>

*Morpho* butterflies have wings with a densely array of scales with complexly variable morphologies; **Figure 1(a)** shows an image of a typical *Morpho didius*. The scales on the dorsal side of the wings can be divided into cover scales and ground scales. The blue ground scales are arranged as a highly reflective array on the ground layer of the wing, while cover scales, which are transparent with a bluish tint, lie above the ground scales to form a second layer (as shown in **Figure**

**1(b)(c)**); both types have a main structure consisting of ridges connected by cross ribs. The major structural difference between the cover and ground scales lies in the density of the cross ribs in between two nearby ridges. The ground scales are much more transparent with a denser layout of cross ribs than cover scales. The scales are flat or slightly curved on the bottom with a typical dimension of approximately 150 μm in length and approximately 50 μm in width (**Figure 1(c)** inset), but each scale has many well-aligned hierarchical longitudinal ridges, which are separated at regular intervals of only one and several tenths of micrometers (as shown in **Figure 1(d)**). Furthermore, all of the layers of lamellas, which are separated by air gaps, stack neatly and run oblique to the base plate with a tilt angle of only a few degrees (as shown in **Figure (e)**). The

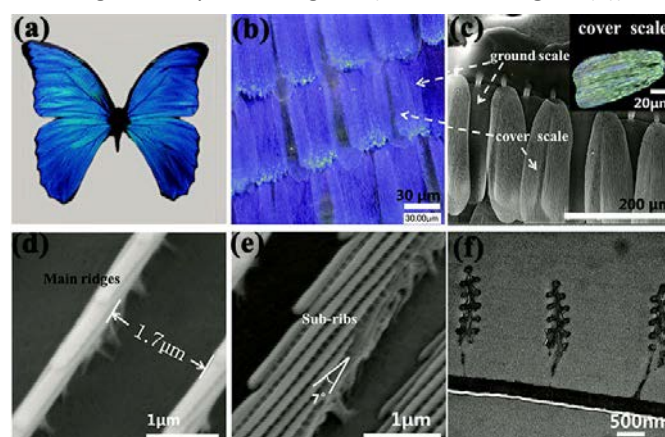


**Figure 1.** (a) The image of a typical *Morpho didius* butterfly, (b) optical image of the scales, (c) the cover scale and ground scale, inset: optical image of a single cover scale, (d) SEM image from the top view of a cover scale, (e) the SEM image of the ground scale, and (f) the TEM image of the ground scale. Reproduced from Ref. 15 with permission from the Royal Society of Chemistry.

<sup>a</sup> National Engineering Laboratory for Modern Silk, College of Textile and Clothing Engineering, Soochow University, Suzhou 215123. E-mail: kqzhang@suda.edu.cn

<sup>b</sup> Department of Physics, Key Laboratory of Micro and Nano Photonic Structures (MOE) and Key Laboratory of Surface Physics, Fudan University, Shanghai, China.

<sup>c</sup> Suzhou Institute of Nano-Tech and Nano-Bionics, Chinese Academy of Sciences, Ruoshui Road 398, Suzhou 215123, China.

lamellas have defined layer thicknesses and inter-layer distances; they are arranged regularly and asymmetrically on both sides of the ridges, extending for tens of nanometers (cross-section cover scale shown in **Figure 1(f)**).<sup>9</sup> The distance between two adjacent lamellas on the same side of ridges is usually in the range of tens of nanometers. Based on extensive study of their microstructures,<sup>10</sup> it can be concluded that the network of longitudinal ridges act as a diffracting grating, contributing to the blue color.<sup>11</sup> The highly iridescent ground scales cause strong diffraction, causing the butterfly wings to appear blue in broad observable directions.<sup>12,13</sup> Meanwhile the cover scales contribute considerably to the wing coloration due to their wavelength-selective reflection and anisotropic optical diffusion.<sup>14,15</sup> The interaction between light and these unique three-dimensional (3D) nanostructures result in effects such as interference, reflection and diffraction, producing optical effects such as color variation when observing from different angles,<sup>16,17</sup> ambient environment or mediums.<sup>18</sup> Aside from *Morpho didius*, other *Morpho* butterfly breeds with notable wing structures include *Morpho sulkowskyi*, *Morpho peleides*, *Morpho Menelaus*, and *Morpho rhetenor*, etc. However, there are only slight differences between the wing structures of the various *Morpho* butterfly subgenera. For example, *Morpho didius* has ground scales and glass scales, while *Morpho rhetenor* has only a single layer of scales with a similar nanostructure to the ground scales of *Morpho didius*. Additionally, the coloration mechanisms of these *Morpho* butterfly wings are also similar. The highly specialized ridges on the wing scales are the most influential optical structural

unit. Wing scale ridges play a crucial role in generating iridescent colors because they are folded into overlapping lamellas, which act as multilayer reflectors and diffraction gratings to interact with incident light and induce complicated optical effects.<sup>19</sup>

A sensor is a type of transducer that detects events or changes in ambient environment by providing a corresponding output. Sensor mounts for pressure, infrared, humidity, gas, displacement, etc. are commonly used in everyday appliances such as the cell phones and health monitoring devices. Sensors typically provide various types of output, such as electrical, mechanical, thermal or optical signals. Most conventional sensors have intrinsic defects which limit their development and practical applications. For example, infrared sensors based on photoelectric detectors exhibit outstanding signal-to-noise ratio and a fast response, but requires cooling, which adds to their size and cost.<sup>20</sup> While, these sensors will be facile to use with lower cost if they are designed based on thermal detectors, but their fabrication requires laborious processing steps, and their sensitivity is limited by active materials.<sup>21</sup>

In contrast, *Morpho* butterfly wings are abundant; although the fine structures that contribute to their color are difficult to fabricate manually, the naturally formed wing structures can be directly applied to devices. The hierarchical tree-like ridges arranged on the scales possess unique structural color effect; color variations are subtle and sensitive to external stimulus. Furthermore, this fast color variation can be easily detected by spectrometers, or even by the unaided eye. A significant amount of research has been dedicated to the design and

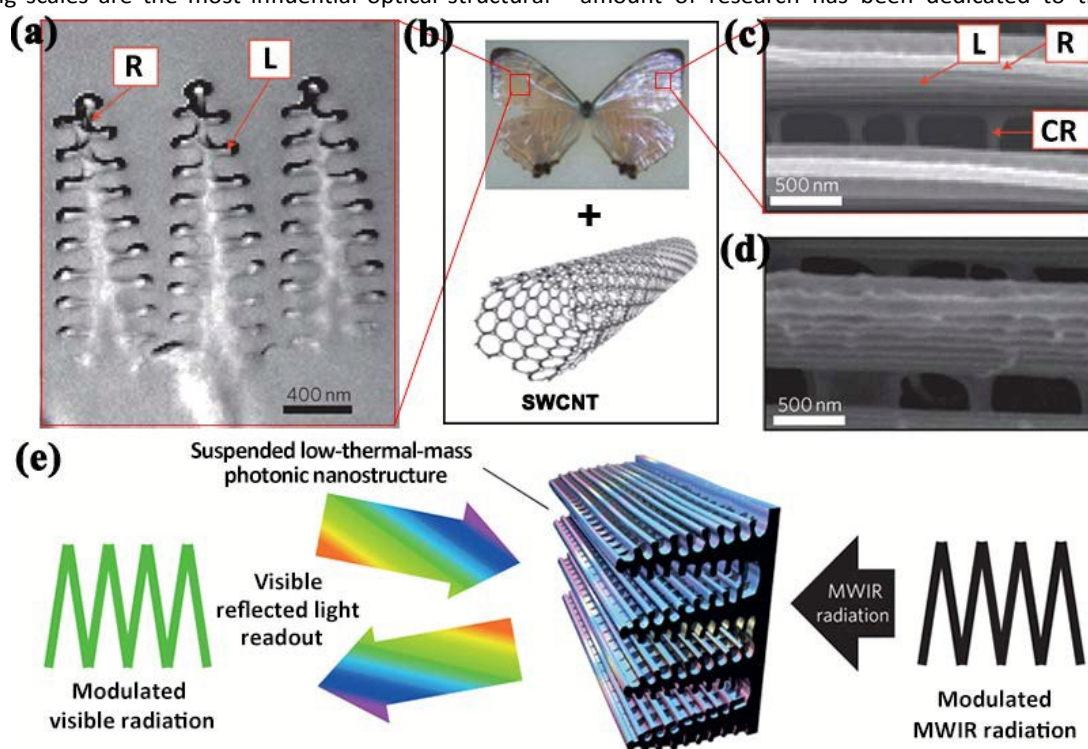


**Figure 2.** The principle of uncooled thermal detection based on the air-filled photonic architecture of iridescent scales of a *Morpho* butterfly. (a) TEM image of a cross-section of the *Morpho* nanostructure. (b) A typical *Morpho sulkowskyi* butterfly and the schematic of SWCNT. SEM images of a portion of a *Morpho* scale before (c) and after (d) modification with SWCNTs. (e) Experimental schematic of MWIR radiation and visible reflected light readout for a *Morpho* nanostructure. R, ridge; L, lamella; CR, crossrib. Reproduced with permission from ref. 28 Copyright 2012, Nature Publishing Group.



synthesis of high preference materials or sensing devices based on the elaborate structures and structure-dependent optical effects of *Morpho* butterfly wings. With improvements in synthesis as well as optimization of their physicochemical properties, *Morpho* wing-based devices have great potential for future applications in many fields.<sup>22, 23</sup>

## 2. Bio-inspired sensors

The fine, subtle nanostructures of *Morpho* wing scales easily deform in response to external stimulus like temperature and humidity. Bio-inspired sensors were designed and fabricated based on the relationship between the structures and their reflected lights. The sensors were made to model the nanostructures found on the butterfly wings, which are responsible for environment-responsive color change. The sensors can be tailored for use in different environments, and made to have high sensitivity and efficiency. Due to the potential of this device, a considerable amount of research has been devoted to this field, resulting in great progress.

### 2.1. Thermal-infrared sensors

Many materials are subject to thermal expansion, changing volume in response to a change of temperature. Due to the

limitations of conventional thermal sensing, such as high cost, complex microfabrication techniques and low spatial resolution, there is great demand for novel thermal-infrared sensors based on new materials or techniques.

It has been long noted that many organisms in nature possess thermal properties attributed to their specific structures.<sup>24-27</sup> Inspired by the properties of *Morpho* butterfly wings, Potyrailo et al.<sup>28</sup> proposed a novel method of preparing outstanding IR-detection sensors by depositing single-walled carbon nanotubes (SWCNTs) on *Morpho sulkowski* butterfly wings, as shown in **Figure 2**. When the wing scales were exposed to mid-wave infrared radiation (MWIR), the temperature of the CNT-doped wings increased and caused the structures to thermally expand, resulting in a change of reflective spectra. The surface-deposited CNTs play a key role in the sensing processes, as their exceptional absorption of IR radiation and high thermal conduction improve the sensitivity of IR detection. Combining the advantages of SWCNTs and the low thermal mass (the ability of a body to store thermal energy) of butterfly wings results in a sensor that possesses a temperature sensitivity of 18–62 mK and heat-sink-free response speed of 35–40 Hz. According to simulation based on finite-difference time-domain (FDTD) method, it was found that the dominant factor of the reflectivity change is attributed to the thermal expansion-induced change in distance between the ridges.

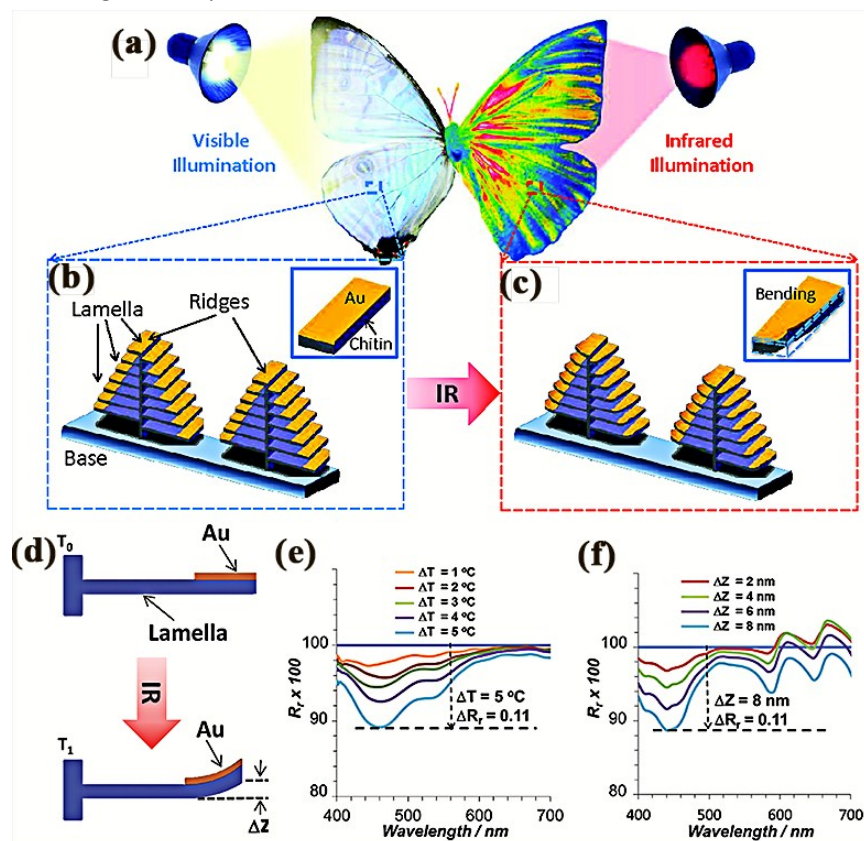


**Figure 3.** Schematic illustration for the IR response of the selectively modified butterfly wing structures. (a) *Morpho* butterfly wing under visible light (left) and IR light (right); (b) 3D nanoarchitecture of modified butterfly wing with Au coating on the edge portion of one lamella under visible light. (c) Schematic of the selectively modified 3D nanoarchitecture of butterfly wings under IR light, with the bending of one lamella layer due to the mismatch in thermal expansion between the Au coating and lamella structure; (d) the schematic illustration of the IR sensing mechanism for the butterfly wing structure modified with Au coating;  $\Delta Z$  is the tip bending distance of the lamella layer under IR radiation. (e) Relative reflectance measured in dependence of  $\Delta T$  (Au thickness is ca. 50 nm). (f) Relative reflectance calculated using FDTD simulation with change in  $\Delta Z$  at the tip of the lamella layers. Reproduced with permission from ref. 29 Copyright 2015, Wiley-VCH.

However, the thermo-optic effect, expansion of the tree-like lamellar structure and decrease of the effective refractive index are all negligible. This is the first time that this method was used to design highly sensitive IR sensor bio-inspired by *Morpho* butterfly wings.

Recently, Deng et al. developed another method to design IR sensors by localizing modification of *Morpho* butterfly wings through physical deposition of gold (Au),<sup>29</sup> as shown in Figure 3. In this work, the sensitivity of the sensor double that of the above-mentioned SWCNT-doped wings. As seen in Figure 1(f) and 2(a), the width of the lamellas increases linearly from top to bottom on the both sides of the ridges. As such, only the edge and top portion of each lamella layer is modified by Au coating during the physical deposition. Because the thermal expansion coefficients (CTE) of Au and chitin (the main substance of the wings) vary significantly, the expansion of the Au-modified portion of the wings is not uniform under IR illumination, as shown in Figures 3(c) and (d). This non-uniform structural expansion induces bending at the edge of the lamellas, resulting in a change in reflectivity or color. Both experimental results and FDTD simulation (Figure 3(e) and 3(f))

verify that the change of optical reflectance is mainly attributed to the bending effect of the lamella layers on the ridges. Using this local deformation mechanism, the sensors can be improved to have a better optical readout.

Synthetic polymers with typical thermal-responsive properties<sup>30-33</sup> have application in a wide variety of fields, including biological diagnosis,<sup>34</sup> drug delivery,<sup>35</sup> and sensing.<sup>36</sup> Combining thermal-sensitive polymers with the structure of *Morpho* butterfly wings has become an intuitive, cost-effective way to design new biomimetic sensors. Xu et al.<sup>37</sup> reported the fabrication of high performance sensors with the ability to tune color over temperature; this fabrication is performed via co-assembly of smart polymers and hierarchical structural *Morpho* butterfly wings. Under certain conditions, the aminated *Morpho* butterfly wings were coated by functional temperature-responsive polymer, poly (N-isopropylacrylamide)-co-acrylic acid (PNIPAm-co-AAc), as shown in Figure 4(a). Due to surface bonding between PNIPAm-co-AAc and aminated *Morpho* butterfly wings, the volume change of PNIPAm-co-AAc induces transformation of the photonic crystal structure. This water-soluble thermo-

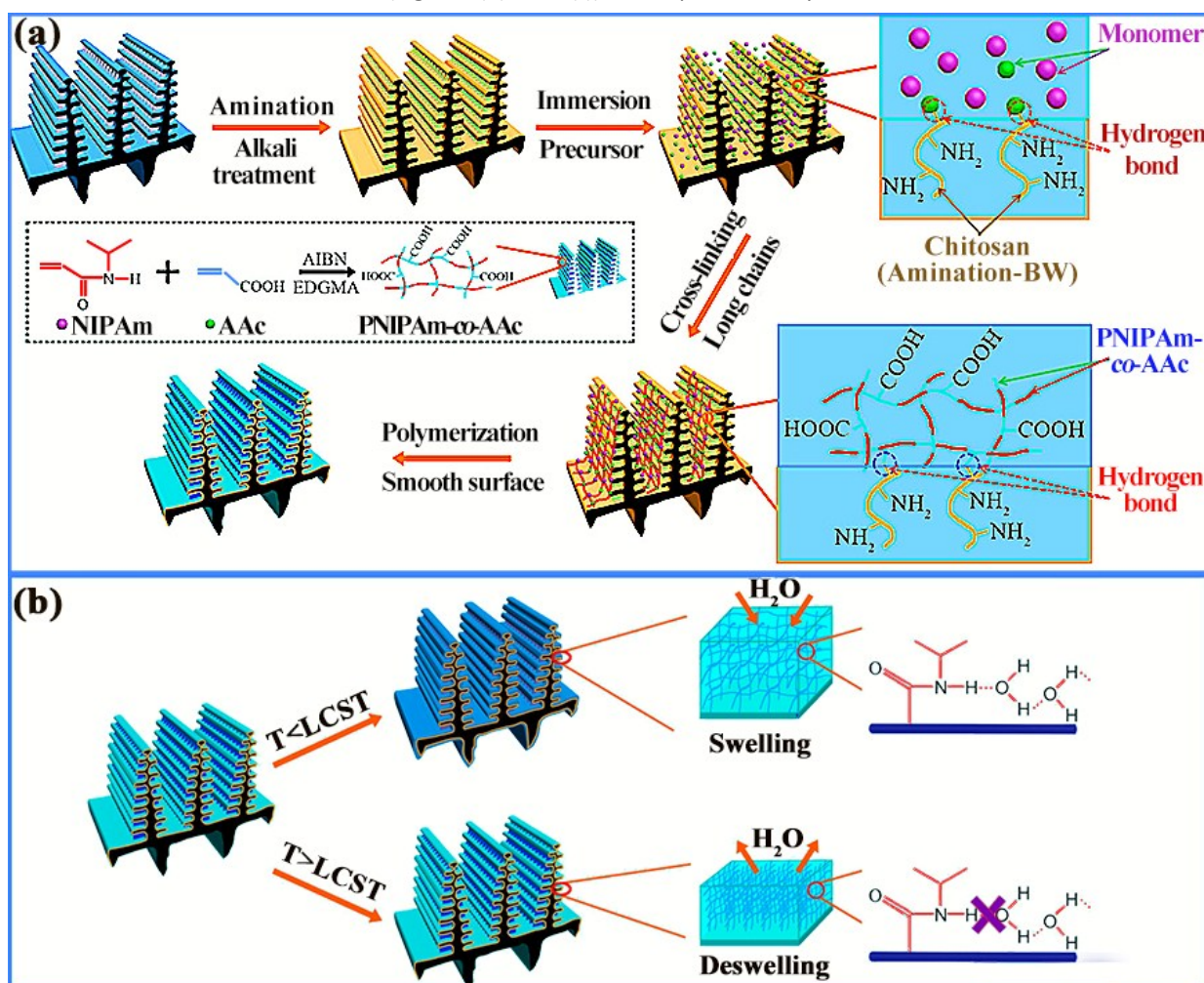


**Figure 4.** (a) Overall synthesis of thermoresponsive photonic structures from *morpho* butterfly wings and mechanism for the temperature responsiveness PNIPAm-co-AAc and *morpho* wings composites. (b) The changing temperature results in the transformation of wing structures by the swelling/de-swelling of the polymer with the enveloping/expelling of water molecules. The expel process of water molecules is marked by purple, a result of few hydrophilically hydrated water molecules continuing interaction with the amide groups in the collapsed state of the polymer. Reproduced with permission from ref.37. Copyright 2015, American Chemical Society.

responsive polymer PNIPAm-co-AAc is known to have a lower critical solution temperature (LCST) at  $\sim 32^\circ\text{C}$ <sup>38</sup>, at which there is a swelling or de-swelling in physical volume change. When the temperature is below the LCST, the cross-linked PNIPAm-co-AAc macromolecules absorb water from the environment and cause the polymer to swell, further increasing the thickness of the wing structures. In contrast, when the temperature is above the LCST, the solvating water can be expelled, resulting in shrinkage of the polymer network volume and a decrease in the thickness of the wing structure; this is illustrated in **Figure 4(b)**. Such deformation causes a color change that is detectable by spectrometer. The mechanism of the hybrid photonic structures' thermal response was theoretically analyzed. Theoretical analysis yielded similar results, showing that the temperature-sensing property of the co-assembling structures is the main factor affecting the temperature-induced changes in PNIPAm-co-AAc. Other effects such as thermal expansion of the butterfly wings, and thermo-optic effects are negligible. Lu et al. reported thermo-responsive photonic materials with hierarchical structures, formed by combining a template of *Morpho* butterfly wings with poly(N-isopropylacrylamide) (PNIPAM) through a chemical bonding and polymerization route.<sup>39</sup> These materials notably showed temperature-induced color tenability, but contrary to previous studies, the reflection peaks red-shifted when temperature increased. This unique phenomenon is caused by changes in refractive index due to the volume change of PNIPAM during temperature increase, and may provide an efficient strategy for the fabrication of stimuli-responsive photonic materials.

The operation mechanisms of thermal/IR sensors based on *Morpho* butterfly wings are classified into three major categories: (a) increasing spacing between the wing scale ridges, (b) tip bending of the lamella layers on the ridges, and (c) structure change induced by coated copolymers. All deformation or the alteration of structure should be

sufficiently distinct to affect the interference or diffraction of light. *Morpho* wing-based thermal/IR sensors have higher performance than conventional detectors, which possess limited response sensitivity.<sup>21</sup> As the unique structures of the wing scales are very compatible with the excellent thermal properties of Au and SWCNTs, butterfly wing-based sensors fabricated by SWCNT doping or Au deposition are not restricted by issues with sensitivity. Furthermore, the fabrication process of sensors based on these naturally-formed structures are simpler than sophisticated semiconductor techniques required to assemble current thermal detectors on the market.

## 2.2. Vapor and solvent sensors

The detection of vapor gas or volatile organic compounds is a significant technology for industries such as military defense and manufacturing, which require work in dangerous and extreme environments.<sup>40-42</sup> With the advance of micro-fabrication techniques, the need for cost-efficient vapor and solvent sensors with better stability and higher sensitivity is becoming increasingly urgent in industry as well as everyday life.

Butterflies wings, especially from the *Morpho* butterfly, display different colors when submerged in vapors or solutions with different refractive indices.<sup>11,16,43-48</sup> Moreover, the displayed colors vary diversely depending on *Morpho* species, submersion time, and certain gas or liquid.<sup>18,49,50</sup> Recent studies have confirmed that the specific color change of *Morpho* butterfly wings can be utilized for vapor sensing. Potyrai et al.<sup>51,52</sup> investigated the mechanisms for optical response of *Morpho* butterfly wings under exposure to different individual vapors, and found that the optical response outperformed that of existing nano-engineered photonic sensors. **Figure 5** illustrates the principle of highly selective vapor response based on the hierarchical structures of the butterfly wing. According to reflective spectra collected

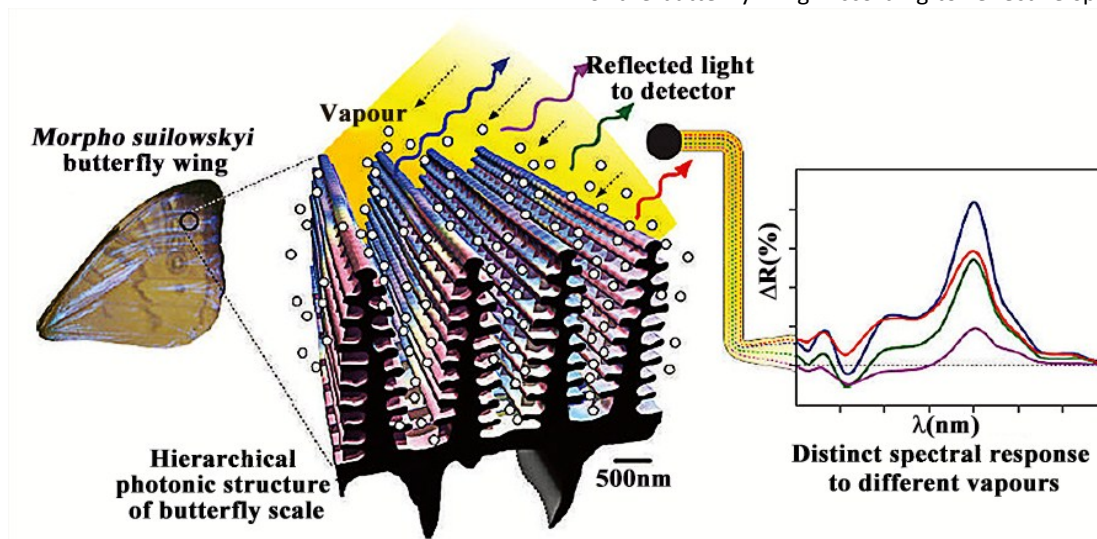


**Figure 5.** Highly selective vapor response based on hierarchical photonic structures is demonstrated by using *M. sulkowskyi* iridescent scales. Measurements of differential reflectance spectra  $\Delta R$  provide information about the nature and concentration of the vapors:  $\Delta R = 100\% \cdot (R/R_0 - 1)$ , where  $R$  is a spectrum collected from scales upon vapor exposure and  $R_0$  is a spectrum collected from scales upon exposure to a carrier gas (dry  $\text{N}_2$ ). Reproduced with permission from ref. 51. Copyright 2007, Nature Publishing Group.



by spectrometer, *Morpho* butterfly wings have a clear and distinct response to the nature and concentration of the vapors surrounding them. The critical analysis of this diverse spectral response suggested that this response is mainly due to a combination of physical absorption and capillary condensation of gas molecules in the gaps of the scales' ridges. The gas concentrations and thicknesses of condensed liquid layer are determined by the pore size of the gaps, surface tension and physicochemical properties of the vapors.

In 2014, Liao et al.<sup>53</sup> demonstrated the application of hierarchical micro/nanostructured *Morpho* butterfly scales to separate and identify nitrogen, methanol and ethanol vapors. This detection was accomplished according to the principle component analysis (PCA) method based on the masses of collected spectra data. Modeling and simulation of the butterfly scales also confirmed that the thickness of the liquid film on scales, which relates to vapor concentration, plays a critical role in reflectance spectra variation.

Several mechanisms have been proposed to explain the *Morpho* butterfly wings' selective response to the different vapors.<sup>49,53,54</sup> In 2013, Potyrailo et al. discovered the presence of a polarity gradient on the *Morpho* butterfly scales surface.<sup>54</sup> In order to validate the existence of a polarity gradient, a suite of complementary techniques were used to assess the chemistry of the ridges at the nanoscale. Assessments included labeling the scales with polarity-sensitive dyes, as well as experimental analysis and simulations exposing *Morpho* scales to various polar vapors. The results of these methods show strong evidence for the existence of a naturally formed surface polarity gradient extending from the polar tops of ridges to their less-polar bottoms. Once the *Morpho* scales are exposed to vapors, gas molecules with different polarities are preferentially adsorbed onto the respective regions of the ridges (Figure 6(a)). This preferential adsorption is expressed in the corresponding spectral regions, as shown in Figure 6(b). Furthermore, using both experimental validation and a vapor-coverage simulation, it was verified that the vapor selectivity is caused by condensed liquid layers on different domains within

the ridge structure. It was concluded that the spectral change is caused by the change in lamella thickness and their refractive index. This study opens opportunity for new gas and liquid sensor design principles, allowing for tailored selectivity in a single sensing unit and the possibility to detect different molecules in complex multiphase vapors. Recently, individual nanofabricated sensors were combined to not only selectively detect separate vapors in pristine conditions, but also quantify these vapors in mixtures.<sup>55</sup>

Similarly, when the wings were immersed in various solvent or liquids, such as water, methanol and ethanol, the medium in the gaps of the scales' ridges shifted from air to solvent with a sharp variation in refractive indices. The tree-like ridges and lamellas were not just covered with condensed liquid layer but almost totally submerged under liquid. Therefore, the reflectance shows a distinct decrease due to the drop in the lamellae-external medium refractive index contrast. Light diffraction and reflection are disturbed, causing a distinct spectrum shift or color change. Both experiments and simulations indicated that the optical properties of *Morpho* butterfly wing scales depend strongly on the varying refractive indices of ambient packing medium, as well as the asymmetry and ordered dimensional variation of the lamellae structure.<sup>56</sup> In summary, the investigation performed above provided confirmation that the *Morpho* butterfly scales possess the sensitivity and selectivity for organic vapors sensing. The experimental theoretical analysis presented here have greatly advanced the understanding of butterfly wing scales' color variation mechanism. Application of these findings will lead to significant selectivity advancements in photonic sensors based on traditional sensing materials.

### 2.3. pH Sensors

Periodically structured photonic crystals with periodicities in the scale of light exhibit photonic band gap properties that can be modulated using the geometries of their precursors.<sup>57</sup> Using specific materials, a type of stimulus-responsive photonic crystal has been exploited for important applications in areas such as thermal and mechanical sensors,<sup>58, 59</sup> biological and chemical sensors,<sup>60-62</sup> pH sensors,<sup>63, 64</sup> humidity and vapor sensors.<sup>65, 66</sup> However, the fabrication of these photonic crystals is complicated with many steps, largely limiting their practical applications. Therefore, sensors based on the periodic photonic structures are unlikely to fulfill the increasing demands for future sensing.

Zhang et al.<sup>67</sup> reported a new class of hierarchically structured photonic crystals (PCs) with color tunability through pH variation, synthesized via the deposition of polymethylacrylic acid (PMAA) onto a *Morpho* butterfly wing template using a surface bonding and polymerization route. First, the *Morpho* butterfly wings were pre-treated with several different solutions to transform the surface chitin of the original butterfly into chitosan, providing the wings with reaction sites for polymerization. Next, a polymerization process with PMAA takes place. The hydrogen bonding between the two functional groups of the bio-template, -COOH of PMAA and -

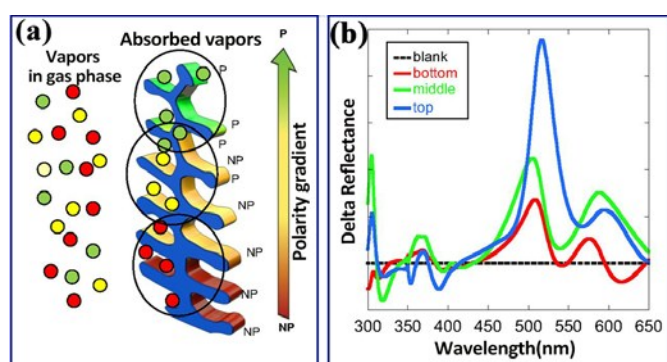


**Figure 6.** The mechanism of the *Morpho* butterfly scales' selective responses to different vapors. (a) The surface polarity gradient of the ridges run from the most-polar ridge tops down to the less-polar ridge bottoms, with different polarity vapors preferentially adsorbed onto the respective regions of the nanostructured ridge. (P=polar; NP=nonpolar) (b) The adsorption of vapors at certain locations along the height of the ridge corresponds to the respective regions in simulated  $\Delta R$  ( $\lambda$ ) spectra. Reproduced with permission from ref. 54. Copyright 2013. National Academy of Sciences, USA.

$\text{NH}_2$  plays a crucial role for uniform coating. The final PMAA hierarchically structured photonic crystals (PMAA-PC) is shown in **Figure 7(a)**. The response properties of the hybrid structures were evaluated by varying the external pH stimulus and monitoring color change as detected by reflective spectra. When the PMAA-PCs were immersed into solutions with varying pH values, the highest reflective peak of each spectrum exhibited an obvious shift and a distinct U transition was observed at, as shown in **Figures 7(c), (d)** and **(e)**.

In investigating the mechanism of the pH-responsive hybrid PMAA-PC sensors, the optical properties of the sensors were found to be mainly due to the interactions between the ions in solution and ions in the hybrid structures. Alkali-treated wing scales exhibit typical swelling or de-swelling behaviors in high or low pH values, respectively, as a result of protonation or deprotonation of the  $-\text{NH}_2$  groups on chitosan. Meanwhile, the swelling/de-swelling behavior of pure PMAA is the opposite. The deprotonation of carboxyl groups inside of PMAA occurs easily in high pH values, while low pH values induce PMMA de-swelling due to decrease in PMAA ionization. These factors cause the final PMAA-PC volume change, which determines the periodic structures of samples and hence, their optical properties.

The pH response of PMAA-PC has a distinct U-shaped curve, which is significant to the swelling/de-swelling mechanism of the PMAA-PC sensors. The U transition point of PMAA-PC-1 is at pH 7.51, and it can be concluded that the volume of the photonic structures is the smallest at the U transition point,

which expands with higher or lower pH values. As shown in **Figure 7(b)**, the expansion of the system in acidic solution is promoted by the breakup of the carboxylate ionic electronic pairs in  $-\text{COO}^-\text{NH}_3^+$ , as well as increasing amounts of positive charges produced by the protonation of primary amino groups. When the photonic structures are placed into an alkali environment (above pH 7.51), the swelling phenomenon is attributed to the deprotonation of the  $-\text{NH}_3^+$  group which results in the dissociation of the electrostatic  $-\text{COO}^-\text{NH}_3^+$  ionic pairs. Additionally, there is an increase of negative charges produced by the deprotonation of carboxyl groups. The combination of these effects in low or high pH values causes the U transition of reflective spectra within a very narrow pH range.

This work is a foundation for future pH sensors. The ability to fabricate responsive photonic crystals with hierarchical structures by combining natural photonic crystals with a pH-responsive polymer provides has great potential for various sensing fields.

#### 2.4. Other sensors

The butterfly wings can be combined with other materials to highly improve its physicochemical properties. Due to the synergistic effects between the different materials, these hybrid structures have tremendous applications towards not only the stimulus-responsive polymers presented above, but also materials such as inorganic magnetic materials for use in magneto-optical response sensors,<sup>15,68</sup> water-splitting

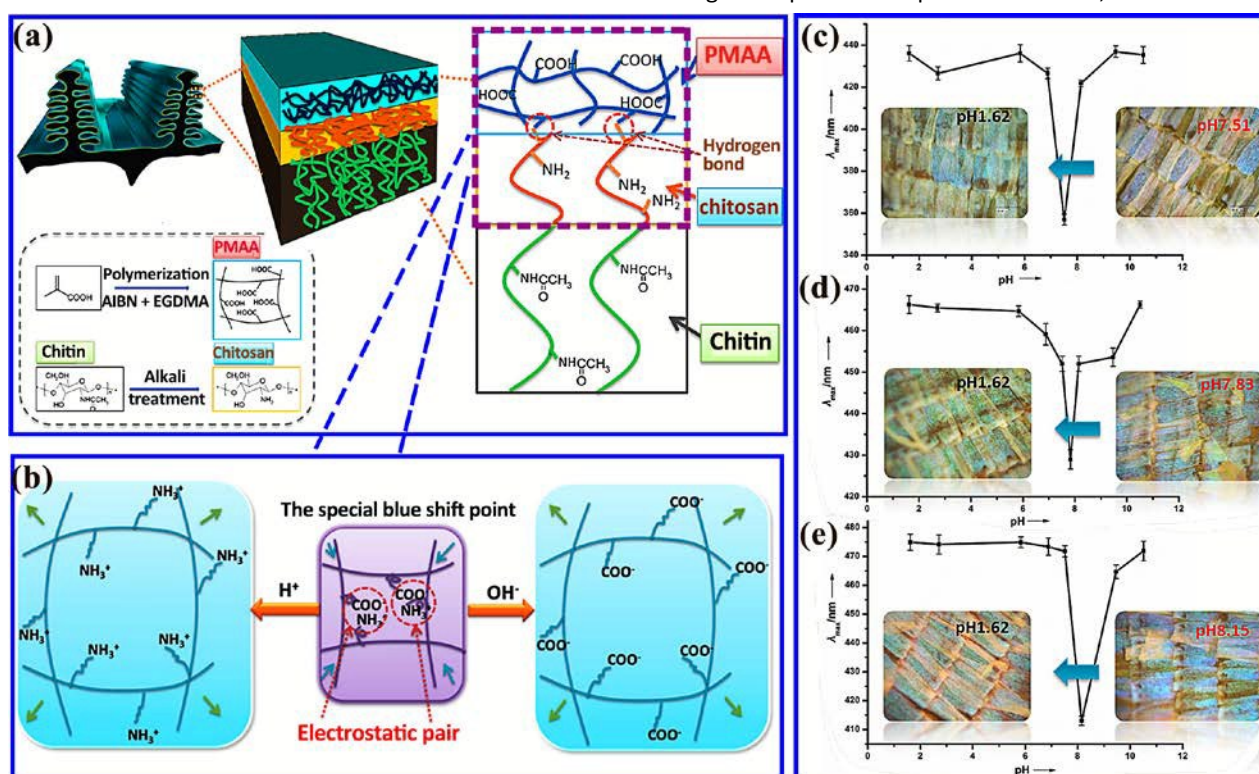


**Figure 7.** (a) Schematic illustration of the formation mechanism for pH-responsive photonic crystals with hierarchical structures (b) Mechanism for the U-shaped pH response of PMAA-PC. Representative spectral responses of (c) PMAA-PC-1, (d) PMAA-PC-2, and (e) PMAA-PC-3 to different pH values, with representative optical images obtained at typical pH values. For the PMAA-PC-1, -2, and -3, the content of PMAA deposited on the samples increases gradually with its monomer concentration in the precursor. Reproduced with permission from ref. 67. Copyright 2013, American Chemical Society.



catalysts,<sup>69</sup> enhanced infrared absorption<sup>70</sup> and photoluminescence,<sup>71</sup> and efficient electrocatalysts.<sup>72</sup> Zhang et al. proposed a simple, sol-gel-based method for fabrication of magneto-photonic crystal (MPC) materials from *Morpho* butterfly wings.<sup>68</sup> The pretreated *Morpho* butterfly wings were immersed in ferric chloride sol-gel solution for coating and then transformed into hematite by calcination to remove the chitin substrates. Magnetophotonic crystal- $\text{Fe}_3\text{O}_4$  (MPC- $\text{Fe}_3\text{O}_4$ ) was obtained by the reduction of as-prepared shelly photonic crystal  $\text{Fe}_2\text{O}_3$  in  $\text{H}_2/\text{Ar}$  atmosphere. The overall process and mechanism is shown in **Figure 8(a)**. Most importantly, the final MPC- $\text{Fe}_3\text{O}_4$  replicas retain the fine structures of the butterfly wings, including nanoscale ribs, and show good magnetic response properties due to expansion under external magnetic fields. A visible color change from a mixture of blue and red to dark yellow can be observed when MPC- $\text{Fe}_3\text{O}_4$  is under external magnetic fields (EMF) of a certain strength, as shown in **Figure 8(b)**. Meanwhile, the experimental curves in **Figure 8(c)** are in accordance with the results of finite-difference time-domain (FDTD) simulation results in **Figure 8(e)**, demonstrating that the MPC- $\text{Fe}_3\text{O}_4$  photonic crystal distorts under the EMF stimulation (**Figure 8(d)**). The synergistic combination of the inorganic polymers and the unique structures of biological creatures provide promise for a future

with unprecedented access to novel high performance, optically superior photonic structures.

In addition to their vivid structural colors, *Morpho* butterfly wings also exhibit anisotropy in the sliding behavior of water droplets on their surfaces.<sup>73, 74</sup> The butterfly wings have excellent superhydrophobic properties<sup>75</sup> due to their composition of naturally formed asymmetric structures, allowing them to remain clean and dry during flight in wet environments. This unique property can be used for the flow control of water droplets,<sup>76-79</sup> with potential applications for superhydrophobic or self-cleaning coating materials.<sup>80, 81</sup>

### 3. Summary and Outlook

Many efficient, sustainable material systems with sophisticated structures can be found across biological species in nature. These structures are the result of billions of years of evolution and enormous pressures from natural selection and competition.<sup>4,82,83</sup> Studying the structure and mechanism of biological systems can inspire the development of high performance materials that lead to superior engineering solutions.<sup>84-87</sup> The investigation, imitation and fabrication of natural biological materials are difficult, but the product of such research often contributes greatly to technological

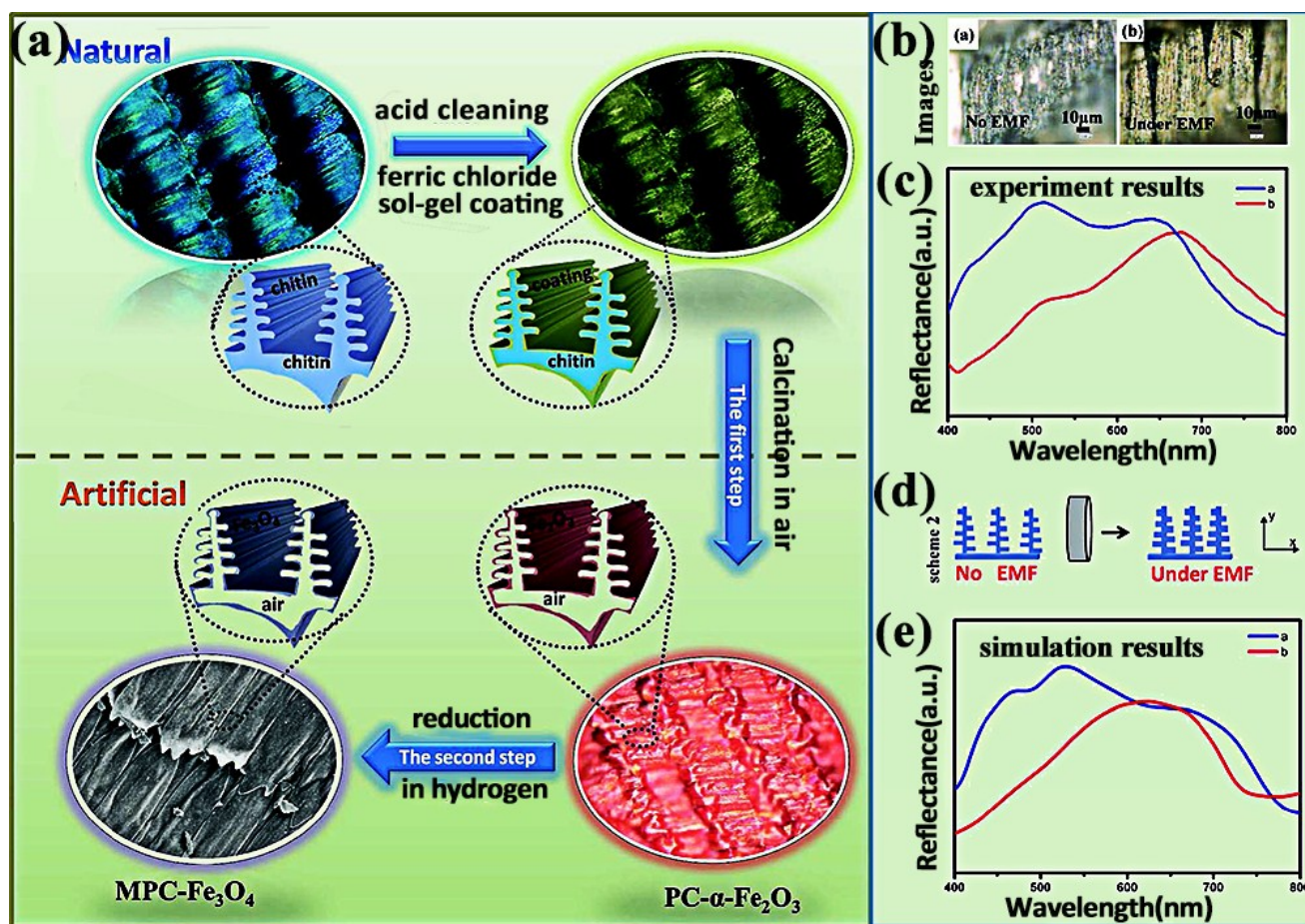


**Figure 8.** (a) Schematic illustration of the process of replicating 3D network magnetophotonic crystals from *Morpho* butterfly wings. (b) Optical images of the sample under no external magnetic field (EMF) (left) and under an EMF (right). (c) The corresponding experimental reflective spectra. (d) Schematic illustration of the changing process under an EMF. (e) FDTD simulation results. Reproduced with permission from ref. 68. Copyright 2012, Wiley-VCH.

advancements.<sup>27, 88-95</sup>

*Morpho* butterflies are a typical representative of commonly researched species with a complex biological system. Scientists across the world have devoted tremendous effort to understand the underlying mechanism of the unique structural coloration on its wings, and to develop promising practical applications based on its structure. A large amount of experimental research and detailed simulations have been performed on the nanostructures of *Morpho* butterfly wings;<sup>23, 96-99</sup> a great deal of strong technical and theoretical support is available for scientists and engineers who wish to design *Morpho* wing-based technology. Based on available research, many researchers have used mature fabrication processes or materials to create technology mimicking the structures of wing scales.<sup>100-104</sup> The sol-gel process is commonly used during biotemplating fabrication; due to its wide accommodation to numerous reagents, easy shape control and mild reaction conditions, it can be developed to synthesize ordered materials templated from natural materials.<sup>105</sup> Replicas of various butterfly wings with conformal structures, including *Morpho*, have been synthesized in this method using various materials, such as europium-doped Y<sub>2</sub>O<sub>3</sub> and TiO<sub>2</sub>,<sup>106</sup> SiO<sub>2</sub>,<sup>107</sup> SnO<sub>2</sub>,<sup>47,108</sup> Mn<sub>2</sub>O<sub>3</sub>,<sup>109</sup> ZnO,<sup>110</sup> ZrO<sub>2</sub><sup>111</sup> and other nanocrystalline multicomponent oxides<sup>112</sup>. Moreover, the nanoimprintation process has been used on butterfly wings templates to create negative or positive structures, greatly simplifying the fabrication process and enabling reproduction of original complex patterns.<sup>113, 114</sup> Vapor phase deposition is a good alternative because of its simple and accurate control over the thickness during deposition. In particular, soft and fragile butterfly wings can be easily utilized to produce exact replicas or modifications with inorganic oxide.<sup>115-118</sup> Additionally, nanocasting lithography combined with electron-beam deposition,<sup>119</sup> focused-ion-beam chemical vapor deposition,<sup>120, 121</sup> plasma etching<sup>122</sup> and many other hybrid processes<sup>123, 124</sup> have been developed to produce materials that mimic wing microstructures. With the advancement of nanofabrication techniques and technologies, emerging tools such as 3D printing, have great potential in precisely and cost-effectively manufacturing systems that mimic delicate natural structures. However, technology based on *Morpho* butterfly wings possesses many non-negligible defects or disadvantages, largely limiting its development and applicability. The main component of the *Morpho* butterfly wings is chitin,<sup>125</sup> which is nondurable and unideal for many rigid environments. Chitin is easily decomposed by microbes in wet environments and certain chemical reagents found in harsh working conditions, posing problems for sensors and other devices based on *Morpho* butterfly wings. Furthermore, due to the fragility and complexity of the nanostructures of butterfly wings, most fabrication processes are unable to produce perfect replicas with good structural integrity. For example, the imprinting technique can produce a multilayered structure of the *Morpho* butterfly wing, but the tree-like microstructures are not retained well.<sup>113</sup> The optical and physicochemical properties of the replicas are inferior to that of the original wings, regardless of fabrication by sol-gel process or other processes. Typically,

current *Morpho* wing-based, bio-inspired sensors cannot operate without the assistance of other professional instruments.

Due to the increasing popularity of natural systems and biomimetics alongside growing need for various cost-effective sensors, tremendous opportunities are available in this particular area of research. The next steps for researchers in this field are the holistic understanding of the function of *Morpho* butterfly wings, as well as development of easy-to-use applications for derivative products.

## Acknowledgements

We gratefully acknowledge the financial support from the National Science Foundation of China under Grant 51073113, 91027039, 51373110 and 11404064, the Natural Science Foundation of the Jiangsu Higher Education Institutions of China under Grant 10KJA540046 and Shanghai Pujiang Program (14PJ1401100). Lei Shi acknowledges the support from the Program for Professor of Special Appointment (Eastern Scholar) at Shanghai Institutions of Higher Learning. We also acknowledge support from the Priority Academic Program Development of Jiangsu Higher Education Institutions (PAPD), Qing Lan Project for Excellent Scientific and Technological Innovation Team of Jiangsu Province (2012) and Project for Jiangsu Scientific and Technological Innovation Team (2013).

## Notes and references

- 1 P. Vukusic, *Phys World*, 2004, **17**, 35-39.
- 2 P. Vukusic and J. R. Sambles, *Nature*, 2003, **424**, 852-855.
- 3 J. Y. Sun, B. Bhushan and J. Tong, *Rsc Advances*, 2013, **3**, 14862-14889.
- 4 P. Andrew Richard, *Journal of Optics A: Pure and Applied Optics*, 2000, **2**, R15-R28.
- 5 S. Berthier, J. Boulenguez and Z. Bálint, *Applied Physics A*, 2006, **86**, 123-130.
- 6 S. Kinoshita, S. Yoshioka and K. Kawagoe, *P Roy Soc B-Biol Sci*, 2002, **269**, 1417-1421.
- 7 P. Vukusic and J. R. Sambles, *Proc. SPIE*, 2001, **4438**, 85-95.
- 8 P. Vukusic and D. G. Stavenga, *Journal of the Royal Society, Interface / the Royal Society*, 2009, **6 Suppl 2**, S133-S148.
- 9 G. I. Mark, Z. Vertesy, K. Kertesz, Z. Balint and L. P. Biro, *Physical Review E*, 2009, **80**, 051903.
- 10 Y. Ding, S. Xu and Z. L. Wang, *Journal of Applied Physics*, 2009, **106**, 074702.
- 11 S. Berthier, E. Charron and J. Boulenguez, *Insect Sci*, 2006, **13**, 145-158.
- 12 P. Vukusic, J. R. Sambles, C. R. Lawrence and R. J. Wootton, *P Roy Soc B-Biol Sci*, 1999, **266**, 1403-1411.
- 13 W. Wang, W. Zhang, W. Chen, J. Gu, Q. Liu, T. Deng and D. Zhang, *Optics Letters*, 2013, **38**, 169-171.
- 14 S. Yoshioka and S. Kinoshita, *P Roy Soc B-Biol Sci*, 2004, **271**, 581-587.
- 15 W. Peng, S. Zhu, W. Zhang, Q. Yang, D. Zhang and Z. Chen, *Nanoscale*, 2014, **6**, 6133-6140.
- 16 S. Kinoshita, S. Yoshioka and J. Miyazaki, *Reports on Progress in Physics*, 2008, **71**, 076401.
- 17 W. Wang, W. Zhang, J. Gu, Q. Liu, T. Deng, D. Zhang and H. Q. Lin, *Scientific reports*, 2013, **3**, 3427.



- 18 W. Wang, W. Zhang, X. Fang, Y. Huang, Q. Liu, J. Gu and D. Zhang, *Scientific reports*, 2014, **4**, 5591.
- 19 M. Bartl, J. Galusha and M. Jorgensen, in *Functional Metal Oxide Nanostructures*, eds. J. Wu, J. Cao, W.-Q. Han, A. Janotti and H.-C. Kim, Springer New York, 2012, vol. 149, ch. 9, pp. 175-207.
- 20 A. Rogalski, *Progress in Quantum Electronics*, 2003, **27**, 59-210.
- 21 A. T. Exner, I. Pavlichenko, B. V. Lotsch, G. Scarpa and P. Lugli, *ACS applied materials & interfaces*, 2013, **5**, 1575-1582.
- 22 P. Tao, W. Shang, C. Song, Q. Shen, F. Zhang, Z. Luo, N. Yi, D. Zhang and T. Deng, *Advanced materials*, 2015, **27**, 428-463.
- 23 W. Zhang, J. Gu, Q. Liu, H. Su, T. Fan and D. Zhang, *Phys Chem Chem Phys*, 2014, **16**, 19767-19780.
- 24 E. O. Gracheva, N. T. Ingolia, Y. M. Kelly, J. F. Cordero-Morales, G. Holloper, A. T. Chesler, E. E. Sanchez, J. C. Perez, J. S. Weissman and D. Julius, *Nature*, 2010, **464**, 1006-1011.
- 25 H. Schmitz, H. Bleckmann and M. Murtz, *Nature*, 1997, **386**, 773-774.
- 26 A. L. Campbell, R. R. Naik, L. Sowards and M. O. Stone, *Micron*, 2002, **33**, 211-225.
- 27 D. Klocke, A. Schmitz, H. Soltner, H. Bousack and H. Schmitz, *Beilstein journal of nanotechnology*, 2011, **2**, 186-197.
- 28 A. D. Pris, Y. Utturkar, C. Surman, W. G. Morris, A. Vert, S. Zalyubovskiy, T. Deng, H. T. Ghiradella and R. A. Potyrailo, *Nature Photonics*, 2012, **6**, 195-200.
- 29 F. Zhang, Q. Shen, X. Shi, S. Li, W. Wang, Z. Luo, G. He, P. Zhang, P. Tao, C. Song, W. Zhang, D. Zhang, T. Deng and W. Shang, *Advanced materials*, 2015, **27**, 1077-1082.
- 30 S. T. Sun and P. Y. Wu, *Journal of Materials Chemistry*, 2011, **21**, 4095-4097.
- 31 D. C. Wu, Y. Liu and C. B. He, *Macromolecules*, 2008, **41**, 18-20.
- 32 F. M. Goycoolea, A. Heras, I. Aranaz, G. Galed, M. E. Fernandez-Valle and W. Arguelles-Monal, *Macromolecular bioscience*, 2003, **3**, 612-619.
- 33 D. N. Robinson and N. A. Peppas, *Macromolecules*, 2002, **35**, 3668-3674.
- 34 T. Lei, R. Manchanda, A. Fernandez-Fernandez, Y. C. Huang, D. Wright and A. J. McGoron, *RSC Adv*, 2014, **4**, 17959-17968.
- 35 D. Schmaljohann, *Adv Drug Deliv Rev*, 2006, **58**, 1655-1670.
- 36 C. Pietsch, R. Hoogenboom and U. S. Schubert, *Angewandte Chemie*, 2009, **48**, 5653-5766.
- 37 D. Xu, H. Yu, Q. Xu, G. Xu and K. Wang, *ACS applied materials & interfaces*, 2015, **7**, 8750-8756.
- 38 X. Z. Zhang, Y. Y. Yang, F. J. Wang and T. S. Chung, *Langmuir: the ACS journal of surfaces and colloids*, 2002, **18**, 2013-2018.
- 39 T. Lu, S. Zhu, J. Ma, J. Lin, W. Wang, H. Pan, F. Tian, W. Zhang and D. Zhang, *Macromolecular Rapid Communications*, 2015, **36**, 1722-1728.
- 40 A. Ponzoni, E. Comini, I. Concina, M. Ferroni, M. Falasconi, E. Gobbi, V. Sberveglieri and G. Sberveglieri, *Sensors*, 2012, **12**, 17023-17045.
- 41 P. L. Wang, Y. M. Fu, B. W. Yu, Y. Y. Zhao, L. L. Xing and X. Y. Xue, *Journal of Materials Chemistry A*, 2015, **3**, 3529-3535.
- 42 R. A. Potyrailo, C. Surman, N. Nagraj and A. Burns, *Chem Rev*, 2011, **111**, 7315-7354.
- 43 W. J. Wu, G. Liao, T. L. Shi, R. Malik and C. Zeng, *Microelectronic Engineering*, 2012, **95**, 42-48.
- 44 K. Kertesz, G. Piszter, E. Jakab, Z. Balint, Z. Vertesy and L. P. Biro, *Applied Surface Science*, 2013, **281**, 49-53.
- 45 Z. W. Han, S. C. Niu, M. Yang, Z. Z. Mu, B. Li, J. Q. Zhang, J. F. Ye and L. Q. Ren, *Rsc Advances*, 2014, **4**, 45214-45219.
- 46 K. Kertesz, G. Piszter, E. Jakab, Z. Balint, Z. Vertesy and L. P. Biro, *Materials science & engineering. C, Materials for biological applications*, 2014, **39**, 221-226.
- 47 F. Song, H. Su, J. Han, J. Xu and D. Zhang, *Sensors and Actuators B: Chemical*, 2010, **145**, 39-45.
- 48 G. Piszter, K. Kertész, Z. Vértésy, Z. Bálint and L. P. Biró, *Optics express*, 2014, **22**, 22649-22660.
- 49 L. P. Biró, K. Kertésza and Z. Vértésy, *Proc. SPIE*, 2008, **7057**, 1-6.
- 50 G. Piszter, K. Kertész, Z. Vértésy, Z. Bálint and L. P. Biró, *Materials Today: Proceedings*, 2014, **1**, Supplement, 216-220.
- 51 R. A. Potyrailo, H. Ghiradella, A. Vertiatichikh, K. Dovidenko, J. R. Cournoyer and E. Olson, *Nature Photonics*, 2007, **1**, 123-128.
- 52 T. A. Starkey, P. Vukusic and R. A. Potyrailo, *MRS Proceedings*, 2014, **1621**, 197-207.
- 53 T. Jiang, Z. C. Peng, W. J. Wu, T. L. Shi and G. L. Liao, *Sensor Actuat a-Phys*, 2014, **213**, 63-69.
- 54 R. A. Potyrailo, T. A. Starkey, P. Vukusic, H. Ghiradella, M. Vasudev, T. Bunning, R. R. Naik, Z. Tang, M. Larsen, T. Deng, S. Zhong, M. Palacios, J. C. Grande, G. Zorn, G. Goddard and S. Zalubovsky, *Proceedings of the National Academy of Sciences of the United States of America*, 2013, **110**, 15567-15572.
- 55 R. A. Potyrailo, R. K. Bonam, J. G. Hartley, T. A. Starkey, P. Vukusic, M. Vasudev, T. Bunning, R. R. Naik, Z. Tang, M. A. Palacios, M. Larsen, L. A. Le Tarte, J. C. Grande, S. Zhong and T. Deng, *Nature communications*, 2015, **6**, 7959.
- 56 G. Liao, H. Zuo, X. Jiang, X. Yang and T. Shi, *Frontiers of Mechanical Engineering*, 2012, **7**, 394-400.
- 57 C. Lopez, *Advanced materials*, 2003, **15**, 1679-1704.
- 58 E. P. Chan, J. J. Walish, A. M. Urbas and E. L. Thomas, *Advanced materials*, 2013, **25**, 3934-3947.
- 59 H. H. Xing, J. Li, J. B. Guo and J. Wei, *Journal of Materials Chemistry C*, 2015, **3**, 4424-4430.
- 60 K. Lee and S. A. Asher, *Journal of the American Chemical Society*, 2000, **122**, 9534-9537.
- 61 W. Hong, X. Hu, B. Zhao, F. Zhang and D. Zhang, *Advanced materials*, 2010, **22**, 5043-5047.
- 62 E. C. Wu, J. S. Andrew, L. Cheng, W. R. Freeman, L. Pearson and M. J. Sailor, *Biomaterials*, 2011, **32**, 1957-1966.
- 63 X. Xu, A. V. Goponenko and S. A. Asher, *Journal of the American Chemical Society*, 2008, **130**, 3113-3119.
- 64 Y. J. Lee and P. V. Braun, *Advanced materials*, 2003, **15**, 563-566.
- 65 Z. H. Wang, J. H. Zhang, J. Xie, C. A. Li, Y. F. Li, S. Liang, Z. C. Tian, T. Q. Wang, H. Zhang, H. B. Li, W. Q. Xu and B. Yang, *Advanced Functional Materials*, 2010, **20**, 3784-3790.
- 66 E. T. Tian, J. X. Wang, Y. M. Zheng, Y. L. Song, L. Jiang and D. B. Zhu, *Journal of Materials Chemistry*, 2008, **18**, 1116-1122.
- 67 Q. Yang, S. Zhu, W. Peng, C. Yin, W. Wang, J. Gu, W. Zhang, J. Ma, T. Deng, C. Feng and D. Zhang, *ACS Nano*, 2013, **7**, 4911-4918.
- 68 W. H. Peng, S. M. Zhu, W. L. Wang, W. Zhang, J. J. Gu, X. B. Hu, D. Zhang and Z. X. Chen, *Advanced Functional Materials*, 2012, **22**, 2072-2080.
- 69 H. Liu, Q. Zhao, H. Zhou, J. Ding, D. Zhang, H. Zhu and T. Fan, *Phys Chem Chem Phys*, 2011, **13**, 10872-10876.
- 70 J. L. Tian, W. Zhang, X. T. Fang, Q. L. Liu, J. J. Gu, T. Deng, Y. H. Wang and D. Zhang, *Journal of Materials Chemistry C*, 2015, **3**, 1672-1679.
- 71 K. L. Yu, S. Lou, J. Ding, D. Zhang, Q. X. Guo and T. X. Fan, *Soft Matter*, 2013, **9**, 2614-2620.
- 72 X. M. Guo, H. Zhou, D. Zhang and T. X. Fan, *RSC Adv.*, 2014, **4**, 3748-3752.
- 73 M. Liu, Y. Zheng, J. Zhai and L. Jiang, *Accounts Chem Res*, 2010, **43**, 368-377.



- 74 Y. M. Zheng, X. F. Gao and L. Jiang, *Soft Matter*, 2007, **3**, 178-182.
- 75 D. Byun, J. Hong, Saputra, J. H. Ko, Y. J. Lee, H. C. Park, B. K. Byun and J. R. Lukes, *Journal of Bionic Engineering*, 2009, **6**, 63-70.
- 76 Y. L. Zhang, H. Xia, E. Kim and H. B. Sun, *Soft Matter*, 2012, **8**, 11217-11231.
- 77 S. C. Niu, B. Li, Z. Z. Mu, M. Yang, J. Q. Zhang, Z. W. Han and L. Q. Ren, *Journal of Bionic Engineering*, 2015, **12**, 170-189.
- 78 G. D. Bixler and B. Bhushan, *Nanoscale*, 2014, **6**, 76-96.
- 79 G. D. Bixler and B. Bhushan, *Soft Matter*, 2013, **9**, 1620-1635.
- 80 S. Nishimoto and B. Bhushan, *Rsc Advances*, 2013, **3**, 671-690.
- 81 G. D. Bixler and B. Bhushan, *Nanoscale*, 2013, **5**, 7685-7710.
- 82 C. Sanchez, H. Arribart and M. M. G. Guille, *Nature materials*, 2005, **4**, 277-288.
- 83 A. L. Ingram and A. R. Parker, *Philosophical transactions of the Royal Society of London. Series B, Biological sciences*, 2008, **363**, 2465-2480.
- 84 F. Xia and L. Jiang, *Advanced materials*, 2008, **20**, 2842-2858.
- 85 E. Dujardin and S. Mann, *Advanced materials*, 2002, **14**, 775-788.
- 86 A. R. Parker and H. E. Townley, *Nature nanotechnology*, 2007, **2**, 347-353.
- 87 M. Kolbe, P. M. Salgard-Cunha, M. R. Scherer, F. Huang, P. Vukusic, S. Mahajan, J. J. Baumberg and U. Steiner, *Nature nanotechnology*, 2010, **5**, 511-515.
- 88 C. Schmidt, *Nature*, 2012, **483**, S37.
- 89 H. N. Zang, S. J. Zhang and K. Hapeshi, *Journal of Bionic Engineering*, 2010, **7**, S232-S237.
- 90 R. Brunner, O. Sandfuchs, C. Pacholski, C. Morhard and J. Spatz, *Laser & Photonics Reviews*, 2012, **6**, 641-659.
- 91 N. A. J. M. Sommerdijk and H. Colfen, *Mrs Bulletin*, 2010, **35**, 116-121.
- 92 H. Yin, B. Dong, X. Liu, T. Zhan, L. Shi, J. Zi and E. Yablonovitch, *Proceedings of the National Academy of Sciences of the United States of America*, 2012, **109**, 10798-10801.
- 93 K. S. Liu and L. Jiang, *Nano Today*, 2011, **6**, 155-175.
- 94 Y. Bar-Cohen, *International Journal of Aeronautical and Space Sciences*, 2012, **13**, 1-13.
- 95 F. P. Barrows and M. H. Bart, *Nanomater Nanotechno*, 2014, **4**, 1-12.
- 96 M. A. Steindorfer, V. Schmidt, M. Beleggratis, B. Stadlober and J. R. Krenn, *Optics express*, 2012, **20**, 21485-21494.
- 97 D. Zhang, W. Zhang, J. J. Gu, T. X. Fan, Q. L. Liu, H. L. Su and S. M. Zhu, *Progress in Materials Science*, 2015, **68**, 67-96.
- 98 R. H. Siddique, S. Diewald, J. Leuthold and H. Holscher, *Optics express*, 2013, **21**, 14351-14361.
- 99 K. Watanabe, T. Hoshino, K. Kanda, Y. Haruyama, T. Kaito and S. Matsui, *Journal of Vacuum Science & Technology B*, 2005, **23**, 570-574.
- 100 G. England, M. Kolbe, P. Kim, M. Khan, P. Munoz, E. Mazur and J. Aizenberg, *Proceedings of the National Academy of Sciences of the United States of America*, 2014, **111**, 15630-15634.
- 101 A. Hache and G. G. Allogho, *Optics Communications*, 2011, **284**, 1656-1660.
- 102 E. Miyako, T. Sugino, T. Okazaki, A. Bianco, M. Yudasaka and S. Iijima, *ACS Nano*, 2013, **7**, 8736-8742.
- 103 K. Chung, S. Yu, C. J. Heo, J. W. Shim, S. M. Yang, M. G. Han, H. S. Lee, Y. Jin, S. Y. Lee, N. Park and J. H. Shin, *Advanced materials*, 2012, **24**, 2375-2379.
- 104 S. Lou, X. Guo, T. Fan and D. Zhang, *Energy & Environmental Science*, 2012, **5**, 9195-9216.
- 105 S. Mann, S. L. Burkett, S. A. Davis, C. E. Fowler, N. H. Mendelson, S. D. Sims, D. Walsh and N. T. Whilton, *Chemistry of Materials*, 1997, **9**, 2300-2310.
- 106 J. Silver\*, R. Withnall\*, T. G. Ireland and G. R. Fern, *Journal of Modern Optics*, 2005, **52**, 999-1007.
- 107 S. Zhu, D. Zhang, Z. Chen, J. Gu, W. Li, H. Jiang and G. Zhou, *Nanotechnology*, 2009, **20**, 315303.
- 108 F. Song, H. Su, J. Han, D. Zhang and Z. Chen, *Nanotechnology*, 2009, **20**, 495502.
- 109 S. Zhu, D. Zhang, Z. Li, H. Furukawa and Z. Chen, *Langmuir : the ACS journal of surfaces and colloids*, 2008, **24**, 6292-6299.
- 110 Y. Chen, X. Zang, J. Gu, S. Zhu, H. Su, D. Zhang, X. Hu, Q. Liu, W. Zhang and D. Liu, *Journal of Materials Chemistry*, 2011, **21**, 6140-6143.
- 111 Y. Chen, J. Gu, D. Zhang, S. Zhu, H. Su, X. Hu, C. Feng, W. Zhang, Q. Liu and A. R. Parker, *Journal of Materials Chemistry*, 2011, **21**, 15237-15243.
- 112 J. P. Vernon, Y. Fang, Y. Cai and K. H. Sandhage, *Angewandte Chemie International Edition*, 2010, **49**, 7765-7768.
- 113 S. H. Kang, T. Y. Tai and T. H. Fang, *Current Applied Physics*, 2010, **10**, 625-630.
- 114 X. N. Zang, Y. Y. Ge, J. J. Gu, S. M. Zhu, H. L. Su, C. L. Feng, W. Zhang, Q. L. Liu and D. Zhang, *Journal of Materials Chemistry*, 2011, **21**, 13913-13919.
- 115 J. Huang, X. Wang and Z. L. Wang, *Nano Lett*, 2006, **6**, 2325-2331.
- 116 G. Cook, P. L. Timms and C. Göltner-Spickermann, *Angewandte Chemie International Edition*, 2003, **42**, 557-559.
- 117 F. Liu, Y. Liu, L. Huang, X. Hu, B. Dong, W. Shi, Y. Xie and X. Ye, *Optics Communications*, 2011, **284**, 2376-2381.
- 118 D. Yong, X. Sheng, Z. Yue, C. W. Aurelia, H. W. Melissa, X. Yonghao, W. Ching Ping and W. Zhong Lin, *Nanotechnology*, 2008, **19**, 355708.
- 119 A. Saito, Y. Miyamura, M. Nakajima, Y. Ishikawa, K. Sogo, Y. Kuwahara and Y. Hirai, *Journal of Vacuum Science & Technology B*, 2006, **24**, 3248-3251.
- 120 K. Watanabe, T. Hoshino, K. Kanda, Y. Haruyama, T. Kaito and S. Matsui, *Journal of Vacuum Science & Technology B*, 2005, **23**, 570-574.
- 121 W. Keiichiro, H. Takayuki, K. Kazuhiro, H. Yuichi and M. Shinji, *Japanese Journal of Applied Physics*, 2005, **44**, L48.
- 122 Q. Shen, J. He, M. Ni, C. Song, L. Zhou, H. Hu, R. Zhang, Z. Luo, G. Wang, P. Tao, T. Deng and W. Shang, *Small*, 2015, **11**, 5705-5711.
- 123 T. S. Kustandi, H. Y. Low, J. H. Teng, I. Rodriguez and R. Yin, *Small*, 2009, **5**, 574-578.
- 124 Y. Gao, Z. Peng, T. Shi, X. Tan, D. Zhang, Q. Huang, C. Zou and G. Liao, *J Nanosci Nanotechno*, 2015, **15**, 5918-5923.
- 125 A. G. Richards, *Ann Entomol Soc Am*, 1947, **40**, 227-240.

This review summarizes the state-of-the-art development of *Morpho* butterfly wings used for various physical and chemical sensors.

